Backward-facing step flow
Experimental and numerical approach

Tatiana G. ELIZAROVA[1], **Irina S. KALACHINSKAYA**[2], **Régine WEBER**[3], **Jacques HUREAU**[3], **Jean-Claude LENGRAND**[4]

[1] *Inst. for Math. Modelling, Russian Acad. of Sci., Miusskaya Square, 4a, Moscow 125047, Russia, telizar@yahoo.com*

[2] *Dept. of Comput. Math. and Inform., Moscow State University, Vorbievy Gory 119899, Russia*

[3] *Lab. de Méca. et d'Energ., ESEM, 8, Rue Léonard de Vinci, 45072 Orléans Cedex 2, France, Regine.Weber@univ-orleans.fr*

[4] *Lab. d'Aérothermique, 1C, Av. de la Rech. Scientifique, 45071 Orléans Cedex 2, France*

Abstract. This investigation concerns a fundamental problem of hydrodynamics, which is the transition from laminar to turbulent flow. The particular case studied here is the flow behind a backward-facing step, which is studied experimentally and theoretically for a range of Reynolds numbers, including laminar and transitive flow regimes. The experiments consisted in using PIV to determine the mean flow behind the step for low Reynolds numbers (between 1000 and 5000). The flow was then simulated numerically using a new system of equations for fluid flows, the Quasi HydroDynamic (QHD) system. The experimental and numerical results are compared as concerns the reattachment length behind the step. The match is very good for laminar flows, and qualitative agreement is found for nonsteady transitional flows.

Key words: PIV, direct numerical simulation, laminar flows, turbulent flows.

1. Introduction

The geometry of the flow studied in this paper is shown in Figure 1. The Reynolds number Re is calculated as Vh/ν, where V is the average speed of the flow at the channel entrance section, h the step height, and ν the kinematic viscosity coefficient. Experiments were performed in an LME-ESEM wind tunnel with low velocity adaptation to determine the mean velocity field behind the step (with PIV) and the length of the recirculation area. The mathematical model used, called the Quasi HydroDynamic (QHD) equation system, is a new approach for describing viscous flows. The QHD system describes the variation of time-space averaged hydrodynamic quantities, i.e., density, velocity, and temperature, instead of the space-averaged quantities of the Navier–Stokes (NS) equations. Another difference from the NS equations is the additional dissipative terms, which are small in steady flows but can be essential in non-steady [3]. The numerical simulation was performed using the QHD system with an approximation of an incompressible viscous isothermal flow, without turbulence model.

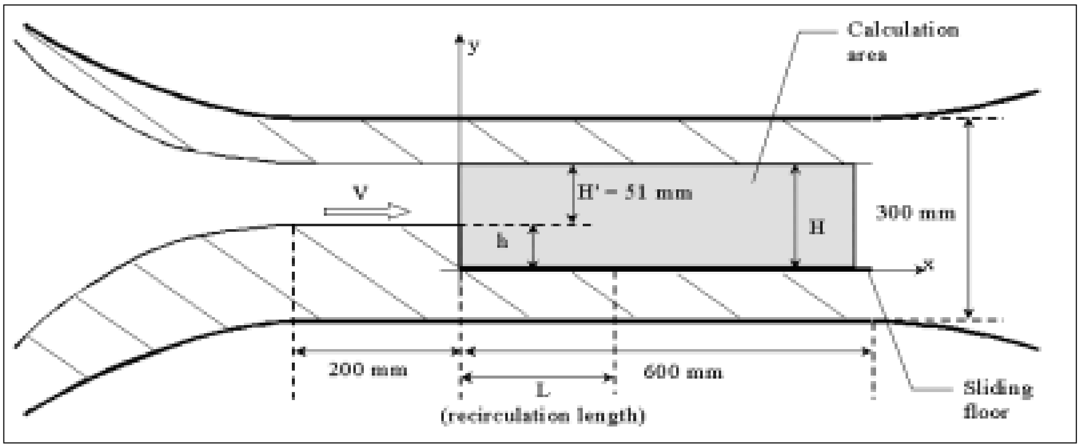

Figure 1: Wind tunnel section and notations.

2. Experimental setup

2.1. Wind tunnel

The experiments were performed in an open air-driven wind tunnel. The existing square section (300 * 300 mm) was adapted to represent a two-dimensional backward-facing step with adaptable step height (Figure 1). The width and the length (800 mm) of the test section were not modified. The electric fan supplies air at velocities up to about 80 m/s in the unobstructed test section. Previous works on this subject [1, 4] pointed out that the reattachment length L of the flow behind the step varies with the Reynolds number Re and the height h of the step: L can be as much as twenty times greater than h. So, in order to visualize the whole flow field (and especially the reattachment area), the test section height H' upstream of the step is set at 51 mm and different step heights between 12 mm and 50 mm are then considered. The length of the test section in front of the step is 200 mm, to get a fully developed flow. The mean velocity obtained with the fan is about 1.4 m/s. Preliminary measurements with a two-component hot-wire anemometer showed that this velocity is stable and uniform. The mean turbulent ratio then measured is less than 0.85 % up to the step. One wall is transparent, for direct visualization, and the others are black. The laser sheet enters the wind tunnel section through a glass window in the upper wall.

2.2. Particule Image Velocimetry (PIV)

The experimental data generated are the two-dimensional velocity components behind the downstep. Tracer particles (mean diameter about 1 μm) are generated and fed into the air line by an oil generator at the settling chamber entrance (velocity about 0.01 m/s). The laser sheet is generated by a double-oscillator laser: a Nd/Yag laser (Spectra Physics 400) adjusted to the second harmonic and emitting two pulses of 200 mJ each ($\lambda = 532$ nm), at a repetition rate of 10 Hz. The laser sheet is developed along an optical arm carrying mirrors and lenses to obtain a 1 mm thick laser sheet with a spread of about 60° around the step. For the experimental data presented here, the flow images are picked up by a CCD with 1008 * 1016 sensor elements (PIVCAM CCD camera), placed perpendicular to the laser sheet. The laser pulses are synchronized with the image acquisition by a TSI synchronizer system driven by InSight-NT^{TM} software. As already stated, the reattachment length can be twenty times the height of the step. The aim of these experimental measurements is to obtain the mean flow behind the step, so we chose to divide the flow area into several visualization areas (80 * 80 mm or 135 * 135 mm) to get good precision in the step wake. This is possible only because the mean velocity field is studied. These subareas overlap by about 10 mm. For all the results presented here, the PIV recordings are divided into interrogation areas corresponding to 64 * 64 pixels. For data post-processing, the interrogation areas overlap by 50 %. The local displacement vector is determined for each interrogation area by statistical methods (auto-correlation). The local flow velocity vector projected onto the laser sheet plane is calculated by InSight from the time between the two illuminations ($\Delta t = 1$ ms) and the magnification at imaging. The post-processing used here is very simple – no more than a velocity range filter.

3. Numerical approach

The Quasi-HydroDynamic (QHD) equations for incompressible viscous flows in the absence of the external forces can be written in index form as

$$\nabla_i u^i = \nabla_i w^i, \tag{1}$$

$$\frac{\partial u^k}{\partial t} + \nabla_i(u^i u^k) + \frac{1}{\rho}\nabla^k p = \nabla_i\ \Pi^{ik}_{NS} + \nabla_i(u^i w^k) + \nabla_i(w^i u^k), \tag{2}$$

$$\frac{\partial T}{\partial t} + \nabla_i(u^i T) = \nabla_i(w^i T) + \kappa \nabla_i T. \tag{3}$$

The Navier–Stokes viscous stress tensor is

$$\Pi^{ik}_{NS} = \nu(\nabla^k u^i + \nabla^i u^k). \tag{4}$$

The mass flux vector in equation (1) is calculated as

$$J^k = \rho(u^k - w^k), \quad \text{where} \quad W^k = \tau(u^j \nabla_j u^k + \frac{1}{\rho}\nabla^k p). \tag{5}$$

In equations (1)–(5) $\rho = Const.$ is the density, ν the kinematic viscosity, κ the heat diffusivity, and τ characterizes the time averaging interval. As $\tau \to 0$, the QHD system reduces to the classical Navier-Stokes equations. We considered plane two-dimensional isothermal flow in the channel of the height H. For the numerical integration of the QHD equations we used the explicit finite-volume algorithm of the second order in space, as described in [3].

4. Results

The first calculations are carried out for laminar flows at Re = 100, 200, 300 and 400 (h/H=0.5). A Poiseuille velocity profile was set at the entrance section. The specified conditions correspond to the experiments of Armaly *et al.* [1], where the reattachment length was measured for laminar planar flows. The algorithm accuracy

and stability vary as $\tau = a/Re$, where a is such that $0.01 \leq a \leq 10$. In all variants we obtained a steady flow regime. The reattachment length L increases almost linearly with Re. For these investigated Re numbers, the flow pattern is practically independent of the smoothing parameter τ and the size of the computational space grid. The history for approaching a steady state regime for $Re = 400$ is given in the stream functions of Figure 2.
The reattachment length for all Re numbers is in good agreement with the experimental data [1]. For $Re = 300$ and 400, the accuracy of the results obtained using the QHD equations exceeds that obtained by the Navier–Stokes equations, which are also given in [1] (Table 1). Here, t is the dimensionless time to reach the steady state regime.

Re	100	200	300	400
t	20	20	60	110
L/h QHD	5.0	8.2	10.1	14.8
L/h [1] exp	5.0	8.5	11.3	14.2
L/h [1] cal	5.0	8.3	8.4	7.8

Table 1: Reattachment length L for laminar flows, $h/H = 0.5$.

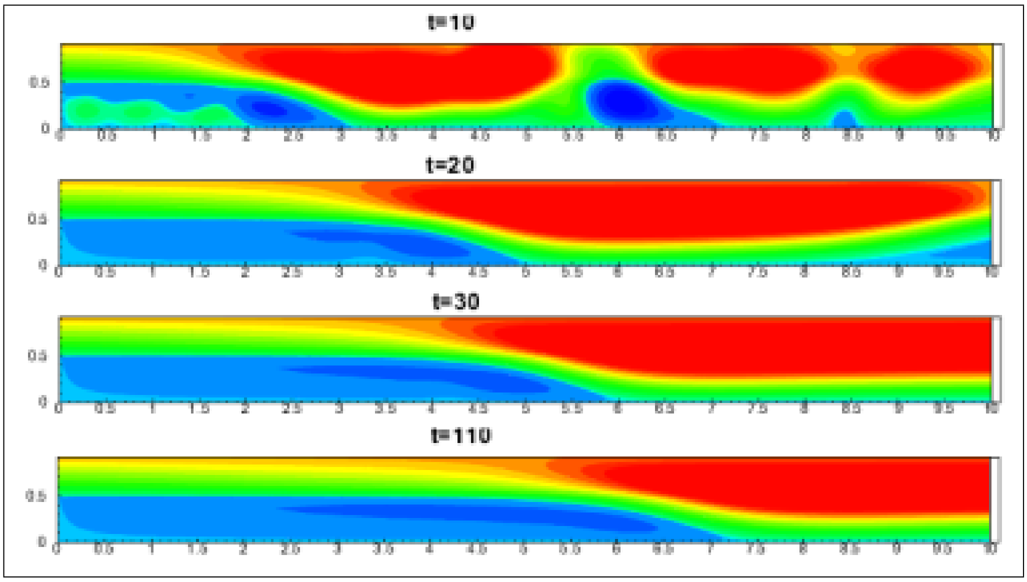

Figure 2: Laminar flow (y/H *versus* x/H), $Re = 400$, $h/H = 0.5$.

A second set of calculations was then generated for larger Reynolds numbers $Re = 1016$ ($h/H \approx 0.19$), 1667 (0.28), 4012 (0.45) and 4667 (0.5), corresponding to the experimental data. A planar velocity profile was set in the entrance section. For turbulent flows, the time τ corresponds to time-averaging interval, which smoothes out the small-scale flow pulsations and resolves large-scale fluctuations. The numerical value of τ was selected on the basis of conformity of the computational and experimental results. Part of the calculations (stream function pictures) for $Re = 4667$ and $\tau = 0.1$ is presented in Figure 4. The reattachment length weakly depends on the value of τ within the limits of a given interval investigated [0.1 - 0.5]. The flow then

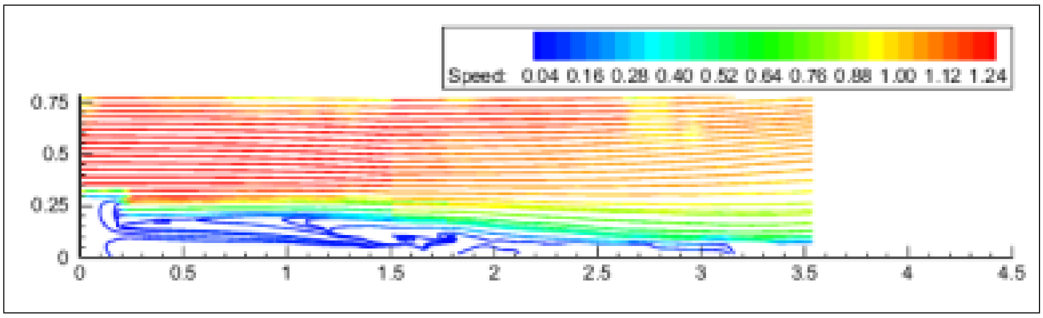

Figure 3: Laminar flow (y/H *versus* x/H), Re=1667, $h/H = 1/3$: mean flow represented with streamlines colored by velocity. $L_{Exp} = 10.8 \pm 0.2$ and $L_{QHD} = 10.6 - 11.0$.

no longer reaches a steady state and the reattachment length is not proportional to Re. The similarity of calculated and measured nonsteady flow structures behind the step can be seen by the previous Figure 4b, where the mean experimental flow pattern is shown. Nonsteady phenomena can be seen behind the step in each PIV image, but these phenomena cannot be studied in this experimental setup (the flow field is too large). In the opinion of the authors, the differences in the reattachment lengths between experiments and calculations stem from the fact that the experimental flow may be somewhat three-dimensional, whereas a pure two-dimensional approach is used in the numerical simulation.
The present numerical and experimental methods and some preliminary results are described in detail in [2].

5. Conclusions

A combined experimental and theoretical study was carried out on backward-facing step flows. To perform the experiments, an aerodynamic tunnel at LME-ESEM was adapted for low Re numbers. The experiments served to find the flow parameters needed for the numerical simulation, and flow visualizations were used to compare the data with the numerical simulation results. These simulations were carried out on the basis of a new system of the equations – QHD system. It is shown that QHD equations can be used to simulate laminar and turbulent flows uniformly without recourse to classical models of turbulence. For laminar flows, the results coincide quantitatively with the experimental data. Here, the value of τ is chosen to obtain the stable numerical algorithm. For turbulent flows, the agreement with experimental data is only qualitative. In this case, the parameter τ corresponds to an averaging scale over time, and should be chosen according to the properties of the investigated flow.
New experiments are under consideration for another wind tunnel. A smaller step with a greater ratio between the tunnel height and its width will be constructed at the LME-ESEM to study the nonsteady problems.

Acknowledgements

This work is supported by grant INTAS N–2000–0617 and by the "Fédération de Recherche" FR776: "Energétique, Propulsion, Espace et Environnement" of Orléans.

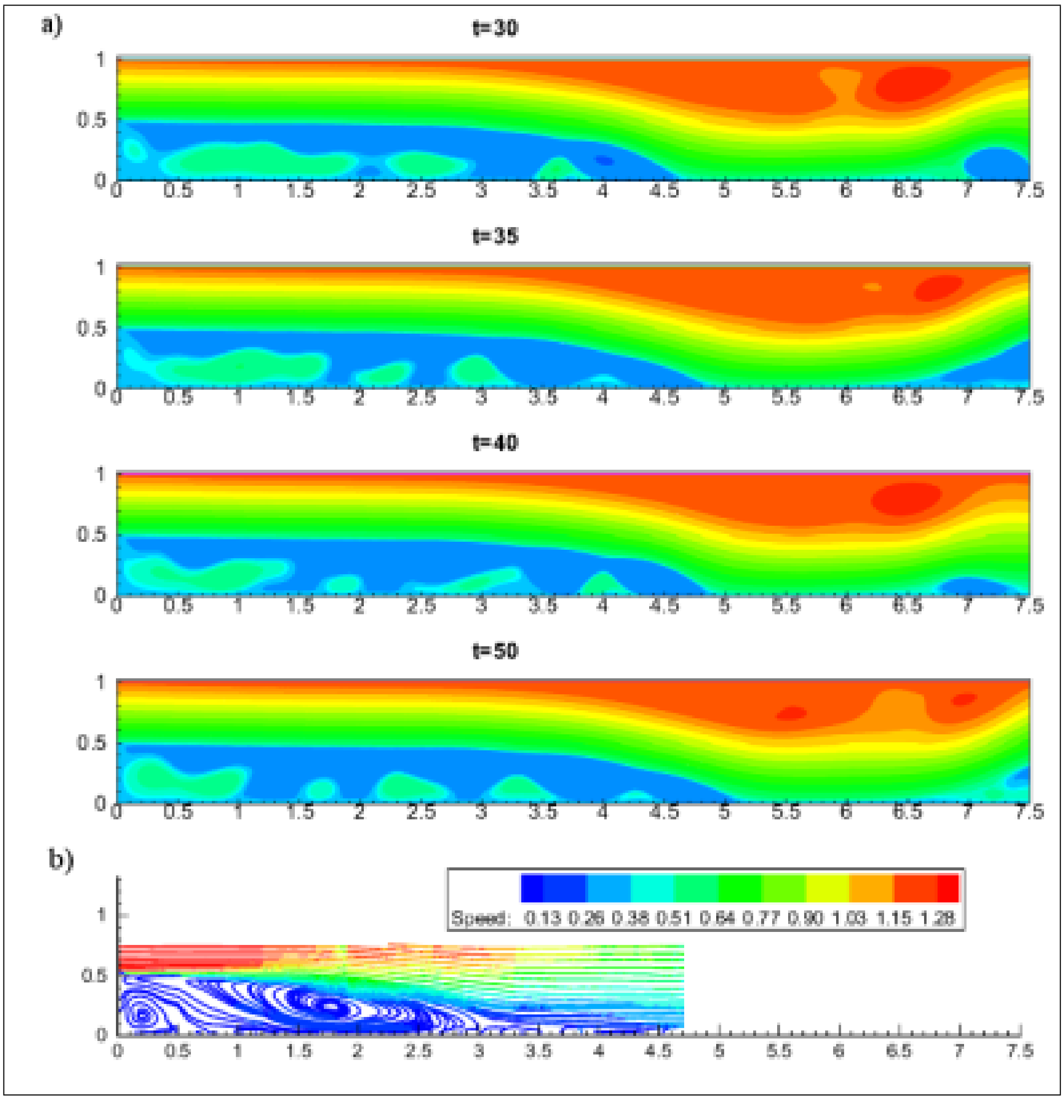

Figure 4: Turbulent flow (y/H *versus* x/H), $Re = 4667$, $h/H = 0.5$. (a) QDH solution and (b) mean experimental flow represented with streamlines colored by velocity.

References

[1] Armaly, B. F., Durst, F., Pereira, J. C. F. and Schonung B., Experimental and theoretical investigation of backward-facing step flow. *J. Fluid Mech.* **127** (1983), 473–496.

[2] Elizarova T. G., Kalachinskaya I. S., Weber R., Hureau J. and Lengrand J.-C., (2001) Ecoulement derriere une marche. Etude expérimentale et numérique. Laboratoire d'Aérothermique CNRS/Orléans (France), R 2001–1 (2001).

[3] Elizarova, T. G. and Sheretov, Yu. V., Theoretical and numerical investigation of quasi-gasdynamic and quasi-hydrodynamic equations. *J. Comput. Mathem. and Mathem. Phys.* **41 (2)** 2001, 219–234.

[4] Perez Guerrero, J. S. and Cotta, R. M., Benchmark integral transform results for flow over a backward–facing step. *Computers & Fluids* **25 (5)** 1996, 527–540.